Studies on the scavengeome of resveratrol

Summary of Ph.D. Thesis

Orinamhe Godwin Agbadua

Doctoral School of Pharmaceutical Sciences
Institute of Pharmacognosy
University of Szeged

Szeged, Hungary
2025

University of Szeged
Doctoral School of Pharmaceutical Sciences
Program of Pharmacognosy
Head: Prof. Dr. Judit Hohmann, DSc

Institute of Pharmacognosy
Supervisor: Prof. Dr. Attila Hunyadi, DSc

Studies on the scavengeome of resveratrol

Summary of Ph.D. Thesis

Orinamhe Godwin Agbadua

Final Exam Committee:
Chair: Prof. Judit Hohmann, DSc
Members: Prof. István Ilisz, DSc
Dr. Gábor Janicsák, PhD

Defense Board:
Chair: Prof. Dr. István Zupkó, DSc
Reviewers: Prof. Dr. Tamás Kőszegi, DSc
Dr. Bálint Lőrinczi, PhD
Members: Dr. Zsuzsanna Schelz, PhD
Dr. Gábor Katona, PhD

Szeged, Hungary
2025

INTRODUCTION

Reactive oxygen and nitrogen species (RONS), which originate from both endogenous (mitochondria, phagocytic cells, peroxisomes, the endoplasmic reticulum, along with several oxidative enzymes like NADPH oxidase, xanthine oxidase and NO synthase) and exogenous sources are key players in both physiological signaling and pathological processes. Reactive oxygen species (ROS) include H_2O_2, $O_2^{\bullet -}$, •OH, RO•, ROO•, and $^1O_2$, while reactive nitrogen species (RNS) include NO, NO_2, and $ONOO^-$.

While low to moderate RONS levels play essential physiological roles, excess RONS cause oxidative stress, damaging lipids, proteins, and DNA, thereby contributing to diseases such as cardiovascular disease and cancer. Biological systems have antioxidant defenses to maintain RONS at optimal levels and mitigate oxidative stress. Antioxidants, which can be enzymatic antioxidants (e.g., SOD, CAT, GPx, PRX, GST) and nonenzymatic compounds (e.g., vitamin C, E, β-carotene, glutathione), work by neutralizing RONS, breaking chain reactions, inhibiting lipid peroxidation, or repairing damage.

The body's intrinsic antioxidants are supplemented by dietary sources rich in polyphenols, such as fruits, vegetables, herbs, and spices. Polyphenols, defined by hydroxylated aromatic structures, primarily exert antioxidant effects by upregulating the Nrf2-ARE pathway and antioxidant enzymes, while downregulating pro-oxidant enzymes like NADPH oxidase and xanthine oxidase (XO). Despite limited direct scavenging ability *in vivo*, the structure of polyphenols allows them to donate or accept electrons, stabilizing free radicals, leading to diverse array of metabolites with greater chemical complexity and unique pharmacological properties. The "scavengeome" describes the full array of metabolites formed when antioxidants neutralize RONS.

Resveratrol (trans-3,4′,5-trihydroxystilbene), is one of the most popular and widely studied dietary polyphenol, found abundant in peanuts, pistachios, cocoa, and a variety of berries. Resveratrol exhibits myriad pharmacological effects such as anticancer, anti-inflammatory, cardioprotective, and neuroprotective effects, which are largely attributed to its antioxidant properties. Like other polyphenols, it operates by influencing both pro-oxidant and antioxidant enzyme systems and can also directly scavenge free radicals due to its chemical structure, resulting in a wide array of oxidized metabolites expectably with modulated pharmacological activities.

AIMS OF THE STUDY

Focusing on the largely overlooked area of structural modifications due to RONS scavenging by antioxidants and their pharmacological implications, the principal aim Ph.D. research, was to leverage performance-based diversity-oriented synthesis to explore the scavengeome of resveratrol after undergoing different oxidative transformations, alongside evaluating the pharmacological actions of these oxidized metabolites.

Consequently, the following objectives were set up:

1. **Preparation of oxidized resveratrol metabolite mixtures.** To achieve this, we aimed to cover the scavengeome of resveratrol using optimized experimental oxidation conditions for each biomimetic and biorelevant oxidant.
2. **Identification of metabolites from these oxidized mixtures**. We aimed to utilize several chromatographic and metabolite profiling techniques to determine the nature of metabolites formed.
3. **Biological evaluation of oxidized mixtures**. We aimed to evaluate the pharmacological activities of the oxidized mixtures as potential inhibitors of several enzymes: angiotensin-converting enzyme (ACE), 15-lipoxygenase (15-LOX) and xanthine oxidase (XO).
4. **Chemical and biological evaluation of isolated compounds**. We aimed to isolate compounds from diverse and bioactive mixtures, identify these oxidized derivatives, and evaluate their biological activities as inhibitors of several enzymes: ACE, 15-LOX, cyclooxygenase-1 and -2 (COX-1 and COX-2) and XO. DPPH scavenging activity and the Oxygen Radical Absorbance Capacity (ORAC) of the oxidized mixtures were also aimed to be evaluated. Lastly, we aimed to develop and apply in silico methodologies in predicting the pharmacokinetic profiles and therapeutic potential.

MATERIALS AND METHODS

Starting material

Resveratrol (>98% pure, as determined by HPLC analysis) was purchased from Career Henan Chemical Co. (Henan province, China).

Preparation of oxidized resveratrol metabolites mixtures

Resveratrol was oxidized by varying concentrations of several biorelevant, and biomimetic oxidants/co-oxidants in microplates. Reactions were monitored at defined intervals, with aliquots analyzed in real-time using laser-assisted rapid evaporative ionization mass spectrometry (LA-REIMS) to obtain metabolite profile of the oxidized mixtures, and bioactivity based on ACE inhibitory screening. Following microplate-based oxidative transformations, optimized oxidative reactions for each experimental set-up were carried out on resveratrol.

Procedures for chromatographic purification

Numerous oxidized metabolites were prepared through oxidative transformation of resveratrol. The compounds were purified by means of normal- or reversed-phase high performance liquid chromatography (HPLC), or normal-phase flash chromatography. Enantiomeric separation was done using chiral-HPLC.

Metabolite profile analysis

The metabolite profile of the oxidized mixtures and pure compounds isolated from these mixtures were done using UHPLC-PDA-ELSD-MS and UHPLC-PDA-CAD-HRMS respectively.

Procedures for structure elucidation

The chemical structure of the obtained pure compounds was elucidated by means of different spectroscopic methods (HRMS, 1D- and 2D NMR). Vibrational circular dichroism (VCD), molecular modeling and calculation of VCD spectra was used to determine the absolute configuration of the enantiomers of interesting compounds.

Biological evaluation of oxidized mixtures and oxidized resveratrol metabolites

Oxidized mixtures were screened for bioactivity by evaluating their inhibitory potential on ACE, 15-LOX, and XO. Isolated compounds were evaluated by testing their potential as inhibitors of ACE, 15-LOX, COX-1 and COX-2, and XO. Based on dose-response studies, the most-potent ACE and XO inhibitors were subjected to enzyme-inhibition kinetic studies to obtain their mode of inhibition, and competitive inhibitors were further subjected to molecular docking simulations. ACE domain-specific inhibitory were also performed. Additionally, the DPPH scavenging activity and the Oxygen Radical Absorbance Capacity (ORAC) of these oxidized metabolites were evaluated. Finally, *in silico* evaluation of the compounds was performed using the ACD/Percepta software, emphasizing Lipinski's rule of five (Ro5) for drug-likeness and augmenting it with the Ertl method to assess intestinal absorption.

RESULTS AND DISCUSSION

Exploring the scavengome of resveratrol

Resveratrol was oxidized using a range of biorelevant, biomimetic, and chemically oxidative models to simulate physiological ROS/RNS scavenging models. Biorelevant *in vitro* models included hydroxyl radical-generating systems (e.g., Fe^{2+}/H_2O_2, metalloporphyrin/H_2O_2, $ONOO^-$), oxidation via xanthine oxidase and the chemical systems with substantial experimental evidence of their suitability for biological oxidative stress (AIBN, AAPH). For biomimetic models, chemical systems involved an oxidation containing an aqueous component in addition to a cosolvent, while related oxidations used anhydrous organic solvents (CH_3CN, CH_3OH, EtOH, DMSO). We therefore considered electron donors ($NaIO_4$, $K_3Fe(CN)_6$, Cu^{2+}, Fe^{2+}/Fe^{3+}), hypervalent iodine reagents (PIDA, PIFA), and agents mimicking peroxynitrite like $NaNO_2$. Most reactions were terminated with glutathione (GSH) to enhance physiological relevance.

Oxidation reactions conducted in microplates resulted in a wide array of metabolite profiles. Real-time monitoring of all oxidative reactions using LA-REIMS revealed a total of 105 and 154 m/z product ions in positive ($[M+H]^+$) and negative mode ($[M-H]^-$), respectively. Key oxidative resveratrol metabolites including dimers (M+H+: 455.1478, M-H-: 453.1337), ethoxy-dimers (M+H+: 501.1919), iodo-substituted and chloro-substituted resveratrol moieties ($M+H^+$: 352.9670, $M+H^+$: 261.0355, respectively) and nitro-substituted derivatives ($M-H^-$: 272.0563) were identified.

To create effective chemical libraries for drug discovery, methods need diversity and high pharmacological success, termed biological performance diversity. Thus, ACE inhibitory activity of the oxidized mixtures was monitored in parallel. Most oxidized mixtures exhibited >97% inhibition at peak activity—substantially higher than unoxidized resveratrol (35–50%). The oxidation of resveratrol led to the formation of multiple oxidized metabolites with improved ability to inhibit the ACE enzyme compared to the parent compound.

A key challenge remains optimizing the balance between broad chemical space coverage and biological relevance. For example, while some oxidation systems expanded chemical space, the resulting oxidized mixtures often lacked significant biological activity as observed in resveratrol oxidation with 8 mM AAPH + 100 mM H_2O_2, which had an 80% inhibition at 4 h, but declined to about 45% inhibition at 21 h 30 min. Thus, we approached this challenge by prioritizing reaction conditions favouring dimer formation ($M+H^+$: 455.1478, $M-H^-$: 453.1337), which were deemed better products for our scavengeome concept and linked to increased bioactivity.

Preparation and evaluation of oxidized resveratrol metabolites

Subsequent to performance-based diversity-oriented resveratrol oxidation, optimal experimental conditions were selected for each oxidative transformation. The resulting oxidized mixtures (Ox1-Ox16) were analyzed by HPLC-PDA to obtain chromatographic fingerprints, and subsequently by UHPLC-PDA-ELSD-MS to obtain a comprehensive overview of their metabolic profile. Comparing their profiles against a diverse array of resveratrol oligomers, the metabolite map of the oxidized mixtures, Ox1–Ox16, showed that oxidized metabolites ranged between 220–570 Da, having *m/z* values signifying resveratrol dimers, ethoxy-substituted derivatives and halogen-substituted derivatives.

To evaluate the pharmacological potential, these chemically diverse oxidized mixtures were screened for inhibitory activity against ACE, LOX and XO – targets known to be modulated by resveratrol. The oxidation of resveratrol resulted in several metabolites with modulated ACE, LOX and XO inhibitory activity when compared to the parent compound as seen in **Table 1**.

Resveratrol scavenges ROS/RNS, forming structurally diverse compounds through mechanisms such as dimerization, C–C coupling, and ring formation—consistent with resveratrol's ability to stabilize radical

intermediates through electron delocalization. Several mixtures exhibited significantly enhanced ACE inhibitory activity compared to resveratrol, notably Ox9 ($ONOO^-$ oxidation), which yielded nearly 100% inhibition and contained trans-ε-/δ-viniferins and a nitro-resveratrol derivative. Halogenated mixtures (Ox5, Ox6) and Fe-catalyzed oxidations also demonstrated improved inhibitory effects on LOX and XO, supporting the therapeutic potential of resveratrol's oxidized scavengeome.

The combined evaluation of the metabolite diversity of these mixtures and their bioactivity served as a guide for the isolation of most bioactive metabolites. Bioactivity results, along with compounds isolated from each mixture, are compiled in **Table 1**.

Table 1. ACE, 15-LOX, and XO inhibitory activities of the oxidized mixtures in comparison with resveratrol, and the compounds isolated from each mixture. Results are expressed as mean ± SEM, n = 3, *: p <0.05 by one-way ANOVA using Dunnett's multiple comparison test to the parent compound, resveratrol. Resveratrol was tested at 90 µM, 40 µM and 100 µM for ACE, 15-LOX and XO inhibition screening respectively, and mixtures Ox1–Ox16 at corresponding concentrations of resveratrol equivalents.

ID	ACE Inh. (%)	LOX Inh. (%)	XO Inh. (%)	Compound isolated
Res.	35.9 ± 1.9	7.0 ± 1.0	49.9 ± 6.9	-
Ox1	51.3 ± 1.2*	45.9 ± 9.1*	42.5 ± 3.3	**1-3**
Ox2	69.9 ± 7.2*	43.8 ± 3.3*	37.6 ± 5.3	**4-7**
Ox3	55.3 ± 3.3*	56.8 ± 7.0*	32.0 ± 2.1*	**6**
Ox4	66.7 ± 6.3*	39.1 ± 4.0*	47.1 ± 1.6	**8-10**
Ox5	87.3 ± 1.6*	42.1 ± 3.8*	55.8 ± 1.8	**5, 8, 11-15**
Ox6	87.7 ± 4.5*	18.9 ± 4.5	67.8 ± 1.8*	**5, 12, 16**
Ox7	64.7 ± 3.5*	2.9 ± 1.4	75.7 ± 4.9*	**5, 13, 14, 17**
Ox8	52.0 ± 7.2*	20.5 ± 3.6	42.3 ± 2.9	**6**
Ox9	94.3 ± 1.9*	31.7 ± 3.8*	63.3 ± 1.6	**2, 6, 19**
Ox10	75.4 ± 3.4*	30. 4 ± 5.6*	46.9 ± 1.1	**4, 18, 19**
Ox11	68.9 ± 0.9*	17.0 ± 1.8	57.5 ± 1.5	**19**
Ox12	48.2 ± 2.3	44.0 ± 3.8*	10.9 ± 2.8 *	**2**
Ox13	64.8 ± 4.0*	34.2 ± 2.5*	29.7 ± 0.5*	**2, 6**
Ox14	86.1 ± 1.2*	29.6 ± 5.1*	31.9 ± 3.2*	**6**
Ox15	59.2 ± 1.7*	12.7 ± 1.0	7.8 ± 0.6*	**6**
Ox16	47.6 ± 4.8	18.5 ± 3.8	2.1 ± 1.6*	**2**

Chemistry of compounds and occurrence in biological environments/systems

The structure of compounds **2**, **4**, **5**, **6**, **16**, **18** and **19**, were previously characterized and by comparing their spectroscopic information with the values in published literatures, they were identified as *trans*-ε-viniferin (**2**), 3β-(3′,5′-dihydroxyphenyl)-2α-(4′′-hydroxyphenyl) dihydrobenzofuran-5-carbaldehyde (**4**), iodo-substituted resveratrol (**5**), *trans*-δ-viniferin (**6**), chloro-substituted resveratrol (**16**), and regioisomeric nitro-derivatives (**18** and **19**). The structure of the other oxidized metabolites were elucidated by employing widely accepted NMR strategies, and included two ethoxy-substituted dimers (**9**, **10**), two open dimers (**1**,

17), several mono- and di-substituted iodine resveratrol derivatives (**12**, **13**, **14** and **15**) and two ethoxy-substituted monomers (**8**, **11**) as seen in **Figure 1**.

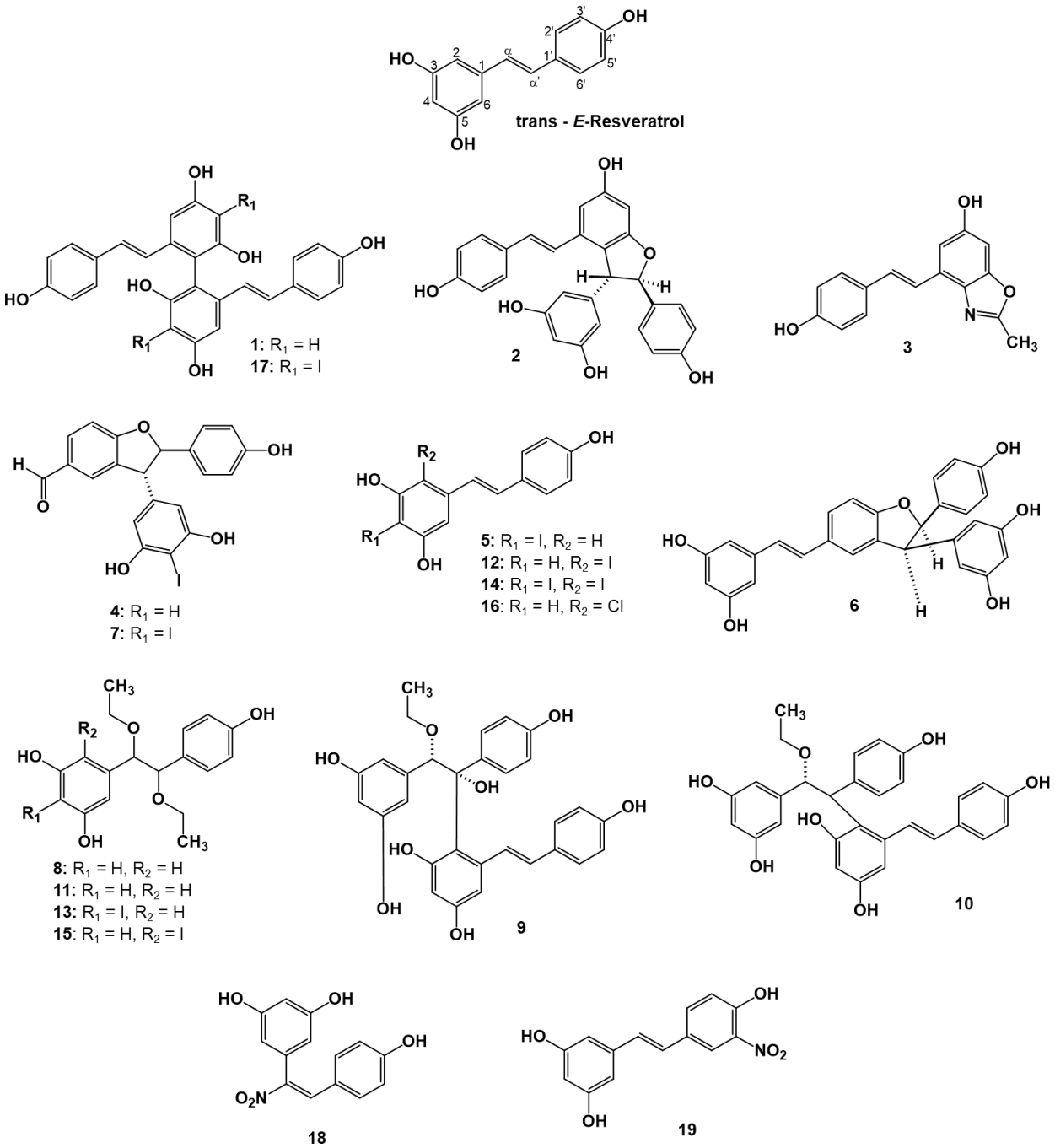

Figure 1: Structures of resveratrol and its metabolites obtained by chemical oxidation (**1**–**19**).

The oxidation of resveratrol led to the isolation of a diverse group of compounds, representing a structural diversity that was expectable from our chemical approach. Compounds **2**, **6**, and **16** are likely products of

resveratrol scavenging free radicals in biological environments. For instance, chlorine substitution seen in compound **16** may be the result of a reaction of a resveratrol radical with chloride ions, which are abundant in intra- and extracellular liquids. Similarly, strong π–π stacking of resveratrol in aqueous media likely promotes radical coupling, forming dimers like compounds **1**, **2**, **4** and **6**, possible in a biological environment under oxidative stress, regardless of the very low concentrations achievable in vivo. Additionally, nitro-derivatives, **18** and **19**, are also expectable products due to the availability of nitric oxide, and its potential to form peroxynitrite in biological systems. Notably, oxidation of resveratrol by XO led to formation of trans-δ-viniferin (**6**), albeit in trace amounts, suggesting a biologically relevant pathway, especially given XO's role in ROS generation under pathological conditions. Compounds **5**, **12**, and **14** expand chemical space towards halogen-substituted derivatives related to compound **16**. Ethoxy substituted compounds **8**–**10** may form when resveratrol oxidizes in ethanol, as during red wine aging.

In silico evaluation of drug-likeness

After elucidating the structure of resveratrol's oxidative metabolites, it became feasible to characterize their drug discovery potential. The principal physicochemical properties relevant to these compounds are summarized in **Table 2**, with the last column delineating the medicinal chemistry rule violations (MedChem issues) associated with any of them.

Lipinski's Rule of Five (Ro5) serves as a guideline to evaluate the drug-likeness of compounds, focusing on parameters such as molecular weight, lipophilicity (logP), hydrogen bond donors, and acceptors, which can help in predicting their absorption and permeation. Ro5 violations (Ro5!) were observed for five compounds (**1**, **9**, **10**, **14**, and **17**), with **17** designated critical due to excessive molecular weight and increased lipophilicity (log *P*), largely from two iodine atoms.

The Ertl method correlates polar surface area (PSA) with intestinal absorption, indicating that compounds with PSA <60 Å² are typically well-absorbed, whereas those with PSA >140 Å² have poor absorption. Consequently, a marginally reduced absorption is predicted for **1**, **10**, and **17**, however for **9**, a minimal absorption level is expected. The isolated resveratrol metabolites were also categorized according to their neutral form or intrinsic aqueous solubility, which is crucial for bioavailability (moderate solubility: <0.1 mg/ml, poor solubility: <0.01 mg/ml). The predicted data demonstrated moderate aqueous solubility for **1**, **2**, **6**, **10**, and **14**, and poor for **17**.

However, it's important to note that while Ro5 provides a useful framework, there are notable exceptions, especially among certain drug classes like antibiotics and antifungals, which often violate these rules yet remain orally active due to specific structural features or active transport mechanisms.

Table 2: Physicochemical characterization of resveratrol and its ROS/RNS-oxidized metabolites (**1**–**19**) using ACD/Percepta suite

Compounds	MW	strongest p$K_{a,acid}$	HBD/ HBA	log*P* / log$D_{7.4}$	TPSA Å²	Solubility mg/ml	MedChem issues
Resveratrol	228.2	9.2	3 / 3	2.8 / 2.8	60.7	1.23	CyP1A2 inhibition
1	454.5	8.5	6[#]/ 6	4.7[#]/ 4.7	121.4[#]	0.01[#]	Ro5! (HBD)
2	454.5	9.2	5 / 6	4.2 / 4.2	110.4	0.08[#]	-
3	267.3	9.0	2 / 4	2.9 / 2.9	66.5	0.17	-
4	348.4	9.2	3 / 5	3.0 / 3.0	87.0	0.28	-
5	354.1	7.8	3 / 3	3.5 / 3.4	60.7	0.35	CyP1A2 inhibition
6	454.5	9.2	5 / 6	4.1 / 4.1	110.4	0.04	-
7	474.3	7.8	3 / 5	3.9 / 3.7	87.0	0.11	-
8	318.4	9.2	3 / 5	2.9 / 2.8	79.2	0.31	-
9	516.5[#]	9.2	7[#]/ 8	3.9 / 3.9	150.8[##]	0.19	Ro5! (MW, HBD), TPSA!
10	500.5[#]	9.2	6[#]/ 7	4.5 / 4.5	130.6[#]	0.02[#]	Ro5! (MW, HBD)
11	318.4	9.2	3 / 5	2.9 / 2.8	79.2	0.31	-
12	354.1	8.1	3 / 3	4.1 / 4.0	60.7	0.24	-
13	444.3	7.7	3 / 5	3.8 / 3.6	79.2	0.17	-
14	480.0	6.6	3 / 3	5.1[#]/ 4.1	60.7	0.04[#]	Ro5! (log*P*)
15	444.3	8.0	3 / 5	4.1 / 4.0	79.2	0.13	-
16	262.7	8.1	3 / 3	3.7 / 3.6	60.7	0.36	-
17	706.3[##]	6.7	6[#]/ 6	6.8[##]/ 5.7	121.4[#]	0.002[##]	Ro5! (MW, HBD, log*P*)
18	273.2	8.8	3 / 6	2.5 / 2.5	106.5	0.5	CyP1A2 inhibition
19	273.2	6.8	3 / 6	3.0 / 2.3	106.5	0.5	CyP1A2 inhibition

[#]moderate or [##]increased violations using classical rule of five or for TPSA ([#]>120 Å², [##]>140 Å²) or for Solubility ([#]<0.1 mg/ml, [##]<0.01 mg/ml).

Given that the ACD/Percepta software's internal database confirmed the experimentally established inhibitory impact of resveratrol on the cytochrome P450 1A2 (CyP1A2) isoenzyme, it was deemed important to evaluate this also for compounds **1**–**19**. *In silico* evaluation of the inhibitory effect of resveratrol and these compounds on the CyP1A2 isoenzyme revealed comparable potential inhibitory effect on CYP1A2 for compounds **5**, **18**, and **19**, similar to the inhibition by resveratrol. Overall, the physicochemical characteristics of the resveratrol metabolites adhere to *in silico* drug-likeness criteria, except for compounds **1**, **9**, **10**, **14**, and **17**. Cytochrome P450 enzymes play a pivotal role in drug metabolism, and inhibition of CYP1A2 can lead to significant drug-drug interactions, affecting the clearance of co-administered drugs metabolized by this enzyme.

Bioactivity of the oxidized metabolites

1. Cardiovascular protective activity

To assess their cardioprotective potential, the oxidized resveratrol metabolites were evaluated for their ACE inhibitory activity, with results compiled in **Table 3**. Most oxidized resveratrol derivatives in this study

showed stronger ACE inhibition than resveratrol. Halogenated derivatives (**5**, **7**, **12**, **14**, **16**, **17**) had improved inhibition in the order of **16** << **5** < **14** ~ **12**, while compounds with ethoxy groups replacing the CH=CH double bond had complete loss of activity (**8**, **11**, **13**, **15**). The reduced effect of **16** may be due to the presence and interaction of chlorine with amino acid residues in ACE's active site. Dimers, especially trans-δ-viniferin (**6**), exhibited enhanced bioactivity, being over 20 times stronger than resveratrol. Monomers connected at CH=CH (**9**, **10**) showed reduced activity compared to aromatic ring-connected counterparts (**1**). Fragmented dimers (**4**, **7**) were also exhibited improved activity.

Table 3. ACE inhibitory activity and ligand-lipophilicity efficiency (LLE) of resveratrol and the isolated pure compounds. Results are expressed as mean ± SEM, n = 3 for % inhibition studies and n = 2 for IC_{50} estimation. % inhibition of the compounds was performed at 90 µM and captopril at 10 µM. *: $p < 0.05$ by one-way ANOVA using Dunnett's multiple comparison test to the parent compound resveratrol. Ligand-lipophilicity efficiency values are calculated by LLE=pIC_{50}-logP using the log*P* values from **Table 2**.

Compounds	**ACE Inh. (%)**	**ACE IC_{50} (µM)**	**LLE**
Resveratrol	38.6 ± 0.6	**185.8** ± 9.1	**0.9**
1	87.4 ± 1.6	**17.5** ± 4.8*	**0.0**
2	81.8 ± 1.0*	**31.8** ± 0.5*	**0.3**
3	33.4 ± 1.0	**106.4** ± 2.0	**1.0**
4	66.9 ± 2.6*	**41.6** ± 2.4*	**1.4**
5	70.9 ± 9.3*	**20.4** ± 2.2*	**1.2**
6	101.0 ± 0.4*	**9.2** ± 0.6*	**0.9**
7	82.0 ± 2.8*	**17.1** ± 1.8*	**0.9**
8	-7.9 ± 2.7*	**>1000**	**-**
9	91.5 ± 0.2*	**36.5** ± 0.8*	**0.5**
10	74.5 ± 5.3*	**33.3** ± 1.5*	**-0.1**
11	-2.9 ± 1.0*	**>1000**	**-**
12	90.5 ± 0.7*	**15.1** ± 1.5*	**0.7**
13	10.8 ± 2.1	**>1000**	**-**
14	81.8 ± 9.3*	**16.2** ± 1.7*	**-0.3**
15	0.5 ± 3.0*	**>1000**	**-**
16	62.4 ± 0.1	**61.6** ± 3.4*	**0.5**
17	71.4 ± 4.9*	**38.8** ± 1.1*	**-2.4**
18	10.7 ± 0.3*	**277.7** ± 7.8	**1.1**
19	28.1 ± 2.8*	**192.4** ± 2.5	**0.7**
Captopril	81.2 ± 1.0*	**0.12** ± 0.1*	**-**

Among the 11 derivatives with IC_{50} values below 50 µM, compounds **4, 5, 6, and 7** demonstrated favorable ligand lipophilicity efficiency (LLE ≥ 0.9), suggesting selective and efficient ACE binding. Based on combined IC_{50}, LLE, and drug-like properties, compounds **6** and **12** emerged as the most promising ACE inhibitor candidates in this study.

Enzyme kinetics study revealed compound **6** as a competitive and compound **12** as a mixed-type ACE inhibitor. As shown in **Table 4**, both compounds preferentially inhibited the C-domain of ACE, which is

primarily responsible for angiotensin II production, making it a crucial target for antihypertensive drug development. Compound **6** preferentially inhibited the C-domain of the enzyme, with a selectivity factor of 2.74.

Table 4: Inhibitory activity of compounds **6** and **12** on the C- and N-terminal domain of rabbit lung ACE. Results are expressed as mean ± SEM, n = 3 for % inhibition and n = 2 for dose-response studies; n. d. = not determined. For both % inhibition and dose-response studies, the substrate concentration [S] = K_M was calculated from initial velocity studies of both substrates; Abz-SDK(Dnp)P-OH; [S] = 79 μM and Abz-LFK(Dnp)-OH; [S] = 33 μM.

Inhibitor	C-domain		N-domain	
	Inhibition (%)[a]	IC_{50} (μM)	Inhibition (%)	IC_{50} (μM)
6	46.3 ± 4.2	17.1 ± 1.2	22.4 ± 0.7	56.4 ± 5.2
12	35.0 ± 3.3	35.1 ± 1.5	12.8 ± 1.9	104.8 ± 3.4
BPPb	80.9 ± 3.1	n. d.	0.6 ± 0.4	n. d.
Angiotensin II	36.8 ± 1.1	n. d.	6.1 ± 1.1	n. d.

[a] Inhibition percentage was determined at 10 μM for angiotensin II, and compounds **6** and **12**, and at 200 nM for BPPb.

Chiral separation showed that *trans*-δ-viniferin (**6**) is a racemic mixture, and biological testing demonstrated the **6a**-(*R,R*) enantiomer had significantly stronger inhibitory activity than its **6b-(***S,S***)** isomer as seen in **Table 5**.

Table 5: ACE inhibitory activity of resveratrol and isolated enantiopure compounds. Results are expressed as mean ± SEM, n = 4 for % inhibition studies and IC_{50} estimation. Inhibition % of the compounds was tested at 50 μM. *: $p < 0.05$ by unpaired t-test assuming Gaussian distribution (parametric test) between the enantiomers.

Compound	ACE Inhibition (%)	ACE IC_{50} (μM)
6	96.3 ± 0.3	10.9 ± 0.1
6a-(*R,R*)	99.4 ± 0.5	8.7 ± 0.6
6b-(*S,S***)**	91.2 ± 0.9	12.1 ± 0.1*

As **6** was shown to be a competitive inhibitor to the ACE, superimposing the best docked orientation of **6a-**(R,R) and **6b-**(S,S) enantiomers with the crystal structure of ACE C- and N-domains (PDB ID: 1O86 and 2C6N, respectively) provided important insights into the difference observed between the bioactivities of **6a-(***R,R***)** and **6b-(***S,S***)** as presented in **Figure 2**. Computational docking showed that binding orientation of **6a-(***R,R***)** to the active site of C-ACE closely resembles that of lisinopril, which may explain its higher inhibitory potential as compared to its enantiomeric pair, **6b-(***S,S***)**. Both enantiomers showed similar binding to the N-domain.

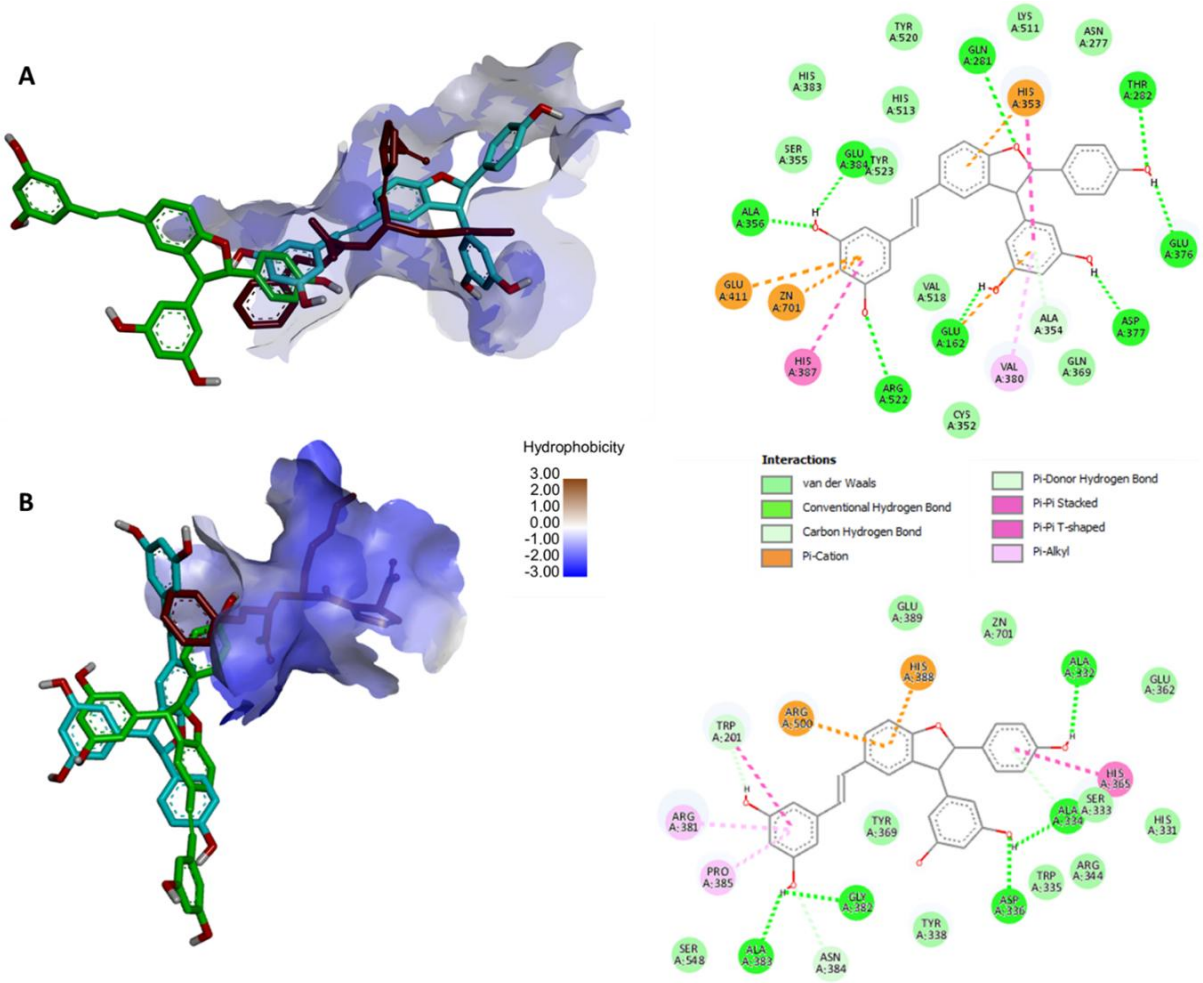

Figure 2. **A**: The best docked position of enantiomers **6a-(*R,R*)** in blue and **6b-(*S,S*)** in green, along with the experimental position of lisinopril (red) in the ACE C-domain active site along with the interaction map of **6a-(*R,R*). B**: The best docked position of enantiomers, **6a-(*R,R*)** in blue and **6a-(*S,S*)** in green, along with the experimental position of lisinopril (red) in the ACE active site along with the interaction map of **6b-(*S,S*)** in the A-chain of ACE N-domain.

2. Anti-inflammatory activities

Angiotensin II activates several inflammatory mediators, leading to the production of proinflammatory cytokines, TNF-α and IL-6. This cascade further underscores the interconnection between ACE inhibitors and inflammation in CVDs. Interdependent of their ability to lower blood pressure, ACE inhibitors may reduce vascular inflammation. The anti-inflammatory potential of the oxidized resveratrol derivatives was evaluated by their inhibition of 15-LOX, COX-1, and COX-2 enzymes (see **Table 6**).

Table 6: Anti-inflammatory activities of resveratrol and compounds **1**–**19**. Positive controls were SC560, Celecoxib, and NDGA for COX-1, COX-2, and 15-LOX, respectively. Results are expressed as mean ± SEM, n = 3. Compounds were tested at 100 μM for LOX % inhibition and 50 μM for COX-1 and COX-2 % inhibition. Dose-response studies were carried out on compounds exhibiting ≥ 70% and 80% inhibition for COX-1 and COX-2, respectively; n.d. = not determined. Ligand-lipophilicity efficiency values were calculated as LLE=pIC_{50}-log*P* using log*P* values from **Table 2**.

Compounds	**COX-1**	**COX-2**	**LOX**
	Inh.(%)/**IC_{50} (μM)/LLE**	Inh.(%)/**IC_{50} (μM)/LLE**	Inh.(%)/**IC_{50} (μM)/LLE**
Resveratrol	98.6 ± 0.2/**2.9** ± 1.0/**2.7**	95.8 ± 1.3/**5.4** ± 0.1/**2.4**	4.3 ± 6.3/> 400
1	65.2 ± 5.2/ n.d.	86.5 ± 2.8/**5.2** ± 0.3/**0.5**	59.8 ± 7.4/**53.4** ± 5.0/**-0.5**
2	80.0 ± 1.4/**9.1** ± 1.6/**0.9**	91.7 ± 2.5/**3.4** ± 0.1/**1.3**	85.8 ± 3.9/**9.7** ± 2.8/**0.8**
3	41.5 ± 4.1/n.d.	72.0 ± 5.2/n.d.	35.0 ± 7.1/**85.7** ± 20.1/**1.1**
4	37.9 ± 3.9/n.d.	80.1 ± 2.5/**19.6** ± 1.4/**1.7**	9.9 ± 6.9/**241.1** ± 21.0/**0.6**
5	73.9 ± 5.3/**21.3** ± 0.7/**1.1**	78.5 ± 2.1/n.d.	18.7 ± 5.0/**120.6** ± 4.9/**0.4**
6	98.6 ± 0.3/**4.7** ± 0.3/**1.2**	92.7 ± 0.9/**5.6** ± 0.6/**1.1**	73.1 ± 4.4/**22.4** ± 8.8/**0.5**
7	37.1 ± 2.8/n.d.	60.6 ± 5.7/n.d.	-14.5 ± 15.8/n.d.
8	16.8 ± 7.9/n.d.	38.9 ± 4.9/n.d.	-2.7 ± 4.7/n.d.
9	29.5 ± 6.0/n.d.	77.7 ± 2.9/n.d.	13.5 ± 14.8/**99.6** ± 5.1/**0.1**
10	65.9 ± 13.1/n.d.	85.2 ± 2.0/**12.2** ± 0.2/**0.4**	-8.6 ± 7.6/n.d.
11	17.4 ± 3.3/n.d.	19.2 ± 6.0/n.d.	-7.4 ± 8.6/n.d.
12	67.3 ± 2.9/n.d.	93.2 ± 0.9/**11.1** ± 0.4/**0.8**	19.9 ± 12.8/**97.2** ± 2.4/**-0.1**
13	29.8 ± 16.4/n.d.	70.2 ± 1.6/n.d.	-11.5 ± 9.0/n.d.
14	26.5 ± 0.6/n.d.	67.1 ± 3.6/n.d.	20.3 ± 5.0/**97.2** ± 2.4/**-1.0**
15	9.5 ± 1.9/n.d.	37.9 ± 3.6/n.d.	-1.2 ± 6.8/n.d.
16	49.1 ± 3.3/n.d.	88.2 ± 1.1/**13.3** ± 0.1/**1.2**	11.6 ± 4.7/**94.4** ± 3.8/**0.3**
17	42.6 ± 17.8/n.d.	60.6 ± 2.8/n.d.	24.2 ± 8.1/174.9 ± 2.2/**-3.1**
18	55.8 ± 4.0/n.d.	48.8 ± 4.2/n.d.	6.2 ± 1.1/>400
19	77.0 ± 1.1/**19.8** ± 0.1/**1.7**	57.5 ± 4.9/n.d.	-0.48 ± 3.8/n.d.
Control	100.4 ± 10.6/0.011 ± 0.1	77.7 ± 1.4/0.5 ± 0.1	80.19 ± 6.4/3.5 ± 0.8

Trans-ε-viniferin (**2**) and *trans*-δ-viniferin (**6**) exhibited the strongest 15-LOX inhibition, with compound **2** being 40 times more potent than resveratrol. Open-ring dimers (**1**, **9**) and iodinated compounds (**5**, **12**, **14**) also showed notable LOX inhibition. 15-LOX appears to play a crucial role in the development of atherogenesis, and targeting this enzyme could provide a feasible strategy in managing CVDs. Most oxidized derivatives were less effective COX inhibitors compared to resveratrol, except for viniferins **2** and **6**. Compound **2** was nearly 3-times more selective for COX-2, unlike resveratrol, which was slightly COX-1 selective. Compound 2's selective COX-2 inhibition allows for effective anti-inflammatory and analgesic effects while minimizing gastrointestinal side effects typically associated with nonselective NSAIDs.

Given the central role of inflammation in CVDs and the well-established link between renin-angiotensin system (RAS) signaling and NF-κB-mediated inflammation, these findings highlight the dual anti-inflammatory and cardioprotective potential of select oxidized resveratrol metabolites, particularly the viniferins.

Anti-inflammatory effects were also assessed using the ligand-lipophilicity efficiency (LLE) metric (see **Table 6**). Relative ligand-lipophilicity efficiency (LLE) values were used since no improved COX inhibition was proven over resveratrol. COX-1 efficacy ranked as **19** > **6** > **5** > **2**, and COX-2 as **4** > **2** > **16** > **6** > **12** > **1**. For LOX, **2** and **6** were identified as the two main enthalpically valuable candidates.

3. Xanthine oxidase inhibition and free radical scavenging activity.

Angiotensin II activates NAD(P)H oxidase in the arterial wall, leading to ROS production and redox signaling cascades that increase oxidative stress. This process plays a critical role in atherosclerosis and cardiovascular events. To evaluate the potential direct antioxidant activity of the compounds in comparison with that of resveratrol, both DPPH scavenging and ORAC assays were employed, with results presented in **Table 7**.

Table 7: XO inhibitory activity along with DPPH scavenging activity and ORAC values of compounds **1**-**19**. Results are expressed as mean ± SEM, n = 3 for % inhibition studies and IC_{50} estimation. *: $p < 0.05$ by one-way ANOVA using Dunnett's multiple comparison test to the parent compound, resveratrol. $n = 2$ for DPPH and 3 = ORAC assay. For XO studies, $n = 4$; due to the large differences, statistical significance was not evaluated for IC_{50} values.

Compounds	**XO** **Inh.(%) / IC_{50} (µM)**	**DPPH** **IC_{50} (µM)**	**ORAC** **(Trolox Equivalent, TE)**
Resveratrol	55.6 ± 1.1/119.4 ± 2.0	27.7 ± 1.4	8.9 ± 0.2
1	30.7 ± 1.7/ n. d.	45.59 ± 1.9	4.8 ± 0.3*
2	69.1 ± 3.1/22.8 ± 6.3	92.1 ± 1.6	15.2 ± 0.5*
3	6.5 ± 1.4*/ n. d.	114.9	7.0 ± 0.2*
4	32.9 ± 1.0/ n. d.	>500	8.6 ± 0.1
5	97.2 ± 4.9*/15.3 ± 1.4	41.0 ± 1.5	9.9 ± 0.5*
6	77.4 ± 2.1/16.4 ± 1.3	340.7 ± 2.1	12.5 ± 0.7*
7	23.0 ± 3.3/ n. d.	>500	9.2 ± 0.5
8	14.4 ± 3.0*/>1000	>500	8.1 ± 0.5
9	31.5 ± 4.8/234.1 ± 4.8	22.6 ± 1.9	9.5 ± 0.3
10	15.1 ± 1.7*/233.3 ± 5.1	53.1 ± 1.5	13.9 ± 0.1*
11	15.0 ± 1.4*/ n. d.	>500	8.1 ± 0.5
12	93.8 ± 1.3*/6.4 ± 0.5	51.7 ± 1.6	12.5 ± 0.7*
13	26.5 ± 1.6/ n. d.	>500	11.0 ± 0.8*
14	45.3 ± 3.0/ n. d.	150.3 ± 1.5	10.5 ± 0.9
15	22.1 ± 0.7*/ n. d.	233.8 ± 5.8	9.3 ± 0.7
16	90.6 ± 4.4*/4.8 ± 0.8	15.8 ± 1.0	9.9 ± 0.5
17	64.4 ± 0.3/ n. d.	87.1 ± 2.9	8.3 ± 0.1
18	87.7 ± 1.8/15.7 ± 0.4	>500	4.7 ± 0.1*
19	66.6 ± 2.1/22.1 ± 0.8	>500	4.5 ± 0.1*
Standard	97.3 ± 0.9*/5.9 ± 0.9	-	-

Halogen substitution influenced antioxidant activity, with chlorine (compound **16**) enhancing DPPH scavenging and iodine (compounds **5**, **12**–**14**) boosting hydrogen atom transfer (HAT) capacity. Additionally, the ethoxy-substituted dimer **10** demonstrated a higher TE value than resveratrol, consistent with findings for other resveratrol dimers lacking a benzofuran ring. Overall, several oxidized resveratrol derivatives were often as effective or exhibited superior antioxidant activity compared to resveratrol in both DPPH and ORAC assays.

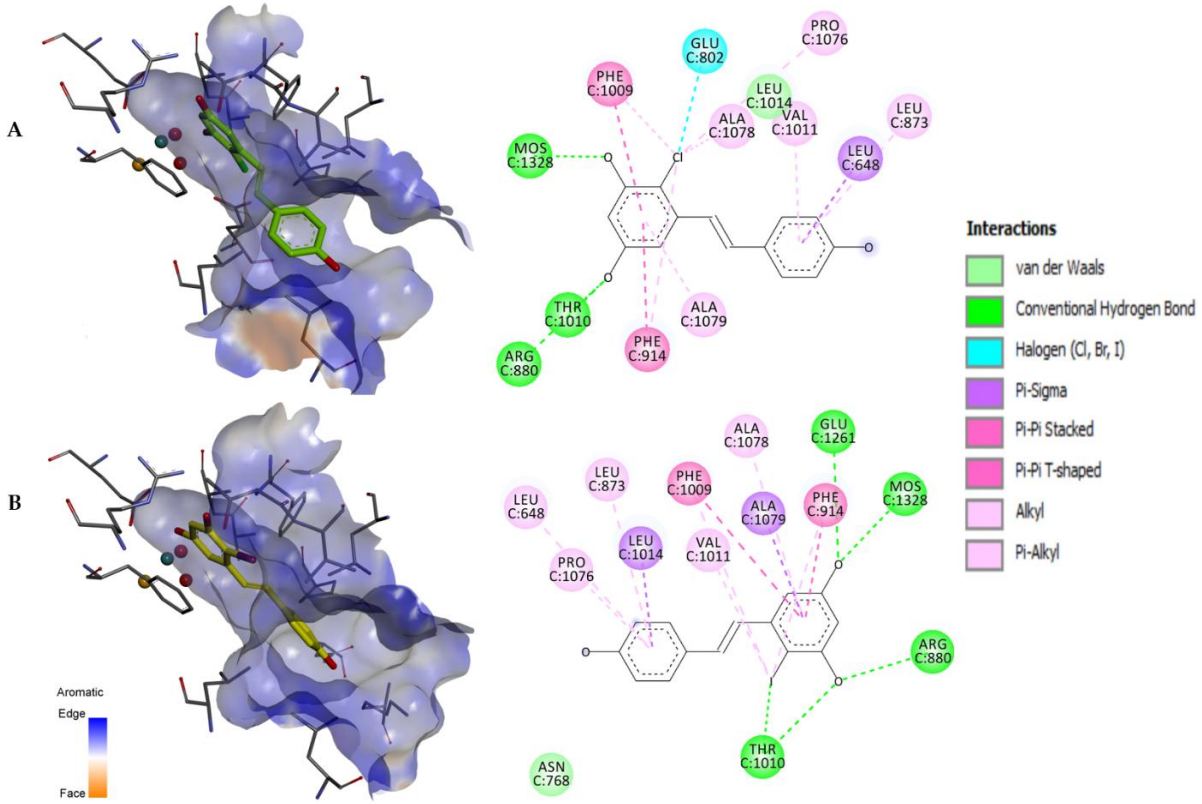

Figure 3. Best-docked poses of compounds **16** (**A**) and **12** (**B**). Three-dimensional orientation and aromatic edge/face receptor surface is shown for both compounds at identical viewing angle and zoom (**left**), along with the 2D interpretation of the ligand–residue interactions with the 3NVY protein (**right**).

In addition to inducing NADPH oxidase, angiotensin II is also known to upregulate xanthine oxidase (XO) expression via ROS. XO-derived ROS and uric acid are implicated in endothelial dysfunction and inflammation, highlighting XO as a key therapeutic target. Therefore, XO inhibitory activity of the compounds was estimated based on their ability to prevent uric acid formation from xanthine. Oxidized resveratrol metabolites, particularly compounds **5, 12,** and **16**, showed markedly enhanced XO inhibition, with **12** and **16** acting as competitive inhibitors comparable to allopurinol as seen in **Table 7**.

Docking studies revealed that compounds **12** and **16** formed key hydrogen bonds with residues critical for XO catalysis, including Mos1328, Glu802, Thr1010, and Glu1261, and showed π–π stacking with Phe914 and Phe1009, stabilizing their orientation at the active site as shown in **Figure 3**. These interactions mirror those seen in established XO inhibitors like quercetin and apigenin, providing strong mechanistic support for the potent inhibitory activity of compounds **12** and **16**.

SUMMARY

Preparation of oxidized resveratrol metabolites

A total of 19 compounds including 7 new compounds were isolated after subjecting resveratrol to a variety of oxidants. Resveratrol oxidation produced structurally diverse metabolites, including dimers, halogenated, ethoxy-substituted, and nitro derivatives, expanding its chemical space.

Biological evaluation of the oxidized metabolites obtained

- Inhibition of ACE: All compounds except those with a loss of the characteristic H-C=C=H had a better activity than resveratrol. Compound **6** (*trans*-δ-viniferin) was the most potent (20 times more active than resveratrol), and enzyme kinetic and domain-specific studies identified it as a competitive inhibitor, preferentially inhibiting the C-domain of the ACE enzyme by a selectivity factor of 2.14. Chiral separation and evaluation revealed the **6a-**(*R*,*R*) as the more potent enantiomer in this regard albeit with a relatively low eudysmic ratio of 1.46.
- Inhibition of 15-LOX: While resveratrol was inactive, several of its oxidized derivatives were inhibitors of this enzyme. *Trans*-ε-viniferin (**2**) was the most active compound (40 times more potent than resveratrol), followed by its isomer, *trans*-δ-viniferin (**6**)
- Inhibition of COX-1 and COX-2: Similar inhibitory action on COX-1 and COX-2 was observed between resveratrol and several oxidized derivatives. In general, compounds inhibited COX-2 better than COX-1, suggesting that the isolated oxidized metabolites might be more specific to COX-2.
- Inhibition of XO: Compounds **5**, **12** and **16** (all halogen-substituted resveratrol derivatives) were the most potent inhibitors of XO. These compounds also inhibited the enzyme competitively, suggesting that the introduction of a halogen substituent to resveratrol played an important role in interacting with the active site of the enzyme. Resveratrol dimers, *trans*-ε-viniferin (**2**) and *trans*-δ-viniferin (**6**), were also better inhibitors than resveratrol, and were identified as mixed-type inhibitors after enzyme kinetic studies.

- Free radical scavenging potential: With a few of the oxidized derivatives having similar DPPH scavenging potential, compounds exhibited better antioxidant activity by hydrogen atom transfer, evident in the Trolox Equivalent values of the compounds from ORAC assay.
- In silico evaluation: Most of the compounds exhibited physicochemical properties within acceptable parameters. Compounds (**1**, **9**, **10**, **14**, **17**) exhibited violations of Lipinski's Rule of Five (Ro5). *In silico* evaluation of the inhibitory effect on cytochrome P450 1A2 (CyP1A2) isoenzyme revealed comparable potential inhibitory effect for compounds **5**, **18**, and **19**, similar to the inhibition by resveratrol.

This study demonstrates that resveratrol's scavenging of biologically relevant ROS/RNS generates diverse metabolites with enhanced pharmacological activities compared to the parent compound, resveratrol itself. As a proof of concept, our approach and findings support a performance-based diversity-oriented exploration of the antioxidant scavengeome as a novel high-hit-rate strategy for drug discovery.

ACKNOWLEDGEMENT

First and foremost, I would like to express my most profound and deepest appreciation to my supervisor, Prof. Attila Hunyadi, for his mentoring, supervision, and encouragement during my Ph.D. study. His immense knowledge, contributions, and guidance helped me sieve through the various challenges that occurred. I am deeply indebted to him.

Secondly, I am thankful to Prof. Dr. Judit Hohmann, the Head of Doctoral School of Pharmaceutical Sciences, and who was the Head of the Institute of Pharmacognosy, at the beginning of my studies. She provided an extremely conducive environment, and her advice and support were important in my study.

I wish to thank all co-authors who contributed their professional expertise. I am grateful to Dr. Norbert Kúsz, Prof. Dr. Gábor Tóth and Dr. Tamás Gáti for the NMR investigations. I am also grateful to Dr. Róbert Berkecz for the assistance provided in the HR-MS measurements. I extend my appreciation to Dr. Emerson Ferreira Queiroz, Prof. Jean-Luc Wolfender, Dr. Laurence Marcourt and Dr. Robin Huber for their contributions towards metabolomic profiling of the oxidized mixtures and pure compounds. I wish to thank Prof. György Tibor Balogh for his help with *in silico* evaluation of the compounds for drug likeness. In addition to helping with this evaluation, I wish to thank him along with Andras Marton and Tamás Karancsi for their help with LA-REIMS measurements. I finally wish to appreciate Dr. Elemér Vass and Prof. Antal Csámpai for their assistance in VCD and absolute configuration determination.

I thank Dr. Meriem Issaadi for taking me under her wing when I first arrived at the department. I owe special thanks to Ibolya Hevérné Herke for her selflessness and her assistance daily during my research work. I appreciate Dr. Gábor Girst for his help with plate reader measurements. I am especially thankful to

other past and current members of the Natural Product Chemical Space Research Group, Institute of Pharmacognosy, University of Szeged.

I wish to thank all members of the Institute of Pharmacognosy for the friendly, wonderful and supportive atmosphere provided during these years. It made my research less tedious and provided me with strength to perform daily tasks needed to complete my study.

Special thanks to the members of my wife, Peace; my brother, Eshi and his family, Jemi, Nathan and Justin; and most importantly, to my mother, whose sacrifice, prayer and encouragement guided me throughout my Ph.D. studies. I am thankful to the Ugbodagas, for their continued love and support. I express my gratitude to the Omamulis for their love and kindness. I am deeply grateful to every family member and friend back in Nigeria for their continued support and encouragement.

I also extend my sincere thanks to all my friends, football and basketball teammates, and everyone I met in Hungary during my program. Their daily encouragement and love strengthened me.

Lastly, I acknowledge the funding provided by the National Research, Development and Innovation Office, Hungary (NKFIH; K119770 and K109293), and TKP2021-EGA-32, implemented with the support provided by the Ministry of Innovation and Technology of Hungary from the NKFIH, financed under the TKP2021-EGA funding scheme. I am also thankful to the Tempus Public Foundation of the Hungarian government for the Stipendium Hungaricum Scholarship and the Bilateral Education Agreement (BEA) Scholarship of the Nigerian government.

LIST OF PUBLICATIONS RELATED TO THE THESIS:

This thesis is based on the following publications:

I. **Agbadua, O.G**., Kúsz, N., Berkecz, R., Gáti, T., Tóth, G., Hunyadi, A. (2022). Oxidized Resveratrol Metabolites as Potent Antioxidants and Xanthine Oxidase Inhibitors.
Antioxidants, *11*, 1832. IF 6.6 (D1)

II. **Agbadua, O.G**., Kúsz, N., Berkecz, R., Vass, E., Csámpai, A., Tóth, G., Balogh, G.T., Marcourt, L., Wolfender, J., Queiroz, E.F., Attila Hunyadi, A. (2025). New Insights into the French Paradox: Free Radical Scavenging by Resveratrol Yields Cardiovascular Protective Metabolites.
Journal of Medicinal Chemistry, *68* (10), 10031-10047 IF 6.8 (D1)

PRESENTATIONS RELATED TO THE THESIS:

I. **Agbadua, O.G**., Hunyadi, A. Lipoxygenase inhibitory activity of oxidized resveratrol metabolite mixtures. The 25th International Symposium on Analytical and Environmental Problems, Szeged, Hungary, October 7-8, 2019. (Oral Presentation)

II. **Agbadua, O.G.**, Hunyadi, A. Studies on oxidized resveratrol metabolite mixtures. 2nd Symposium of Young Researchers on Pharmacognosy. Szeged, Hungary. February 4, 2021. doi: 10.14232/ syrpharmacognosy.2021.a2 (Oral presentation)

III. **Agbadua, O.G.**, Kúsz, N., Huber, R., Marcourt, L., Wolfender, J., Queiroz, E.F., Hunyadi, A. Insight into biomimetic oxidized resveratrol metabolite mixtures. 69th International Congress and Annual Meeting of the Society for Medicinal Plant and Natural Product Research (GA). Planta Med 2021; 87(15): 1253 Bonn, Germany 5-8 September, 2021. doi: 10.1055/s-0041-1736792 (Oral Presentation)

IV. **Agbadua, O.G.**, Hunyadi, A. Studies on biomimetic oxidized resveratrol metabolite mixtures. 3rd Symposium of Young Researchers on Pharmacognosy. Szeged, Hungary, February 3-4, 2022. doi: 10.14232/syrpharmacognosy.2022.a2 (Oral presentation)

V. **Agbadua, O.G.**, Kúsz, N., Gáti, T., Tóth, G., Hunyadi, A. Biomimetic oxidized resveratrol metabolite mixtures. Fiatal Gyógynövénykutatók Fóruma. Budapest, Hungary, June 17, 2022. (Oral Presentation)

VI. **Agbadua, O.G.**, Kúsz, N., Berkecz, R., Gáti, T., Tóth, G., Huber, R., Marcourt, L., Wolfender, J-L., Queiroz, E.F., Hunyadi, A. Exploring the Scavengome of Resveratrol: A Performance-Based Diversity-Oriented Drug Discovery Approach. 2nd Biomedicine and Health PhD Students Congress, Rijeka, Croatia, May 16 - 18 2024 (Oral presentation)

VII. **Agbadua, O. G.**, Kúsz, N., Berkecz, R., Marton, A., Karancsi, T., Gáti, T., Tóth, G., Balogh, G. T., Huber, R., Marcourt, L., Wolfender, J.-L., Queiroz, E. F., Hunyadi, A. French paradox: Exploring the biological relevance of the scavengome of resveratrol. 5th Symposium of Young Researchers on Pharmacognosy. Szeged, Hungary, July 23, 2024. doi: 10.14232/syrpharmacognosy.2024.a3 (Oral presentation)

OTHER PUBLICATIONS:

I. Hunyadi, A., **Agbadua, O. G**., Takács, G., Balogh, G. T. (2023). Scavengome of an Antioxidant. I*n Vitamins and Hormones*, Litwack, G., Ed.; Academic Press: Cambridge, MA, USA, Volume 121, pp. 81–108. IF 2.7 (Q2)

II. Yazdani, M., Barta, A., Berkecz, R., **Agbadua, O. G.,** Ványolós, A., Hohmann, J. Pholiols E–K, Lanostane-Type Triterpenes from *Pholiota populnea* with Anti-Inflammatory Properties. *Phytochemistry* (2023) *205*, 113480 IF: 4.1 (Q1)

III. Ahmed, S.H.H., Gonda, T., **Agbadua, O.G**., Girst, G., Berkecz, R., Kúsz, N., Tsai, M.-C., Wu, C.-C., Balogh, G.T., Hunyadi, A. Preparation and Evaluation of 6-Gingerol Derivatives as Novel Antioxidants and Antiplatelet Agents. *Antioxidants* (2023) *12*, 744. IF: 6.6 (D1)

IV. Dávid, C.Z.; Kúsz, N.; **Agbadua, O.G**.; Berkecz, R.; Kincses, A.; Spengler, G.; Hunyadi, A.; Hohmann, J.; Vasas, A. Phytochemical Investigation of *Carex praecox* Schreb. and ACE-Inhibitory Activity of Oligomer Stilbenes of the Plant. *Molecules* (2024) *29*, 3427. IF: 4.6 (Q2)